The Inferior Right Atrial Isthmus: Further Architectural Insights for Current and Coming Ablation Technologies

JOSÉ ANGEL CABRERA, M.D., PH.D.,* DAMIAN SÁNCHEZ-QUINTANA, M.D., PH.D.,† JERÓNIMO FARRÉ, M.D., PH.D., F.E.S.C.,* JOSÉ MANUEL RUBIO, M.D.,* and SIEW YEN HO, PH.D., F.R.C.PATH, F.E.S.C.‡

From the *Servicio de Cardiología, Fundación Jiménez Díaz, Universidad Autónoma de Madrid; †Departamento de Anatomía Humana, Facultad de Medicina, Universidad de Extremadura, Badajoz, Spain; and ‡National Heart and Lung Institute, Imperial College, and Royal Brompton and Harefield NHS Trust, London, UK

Morphology and Structure of the Inferior Right Atrial Isthmus. ***Background:*** **Although linear ablation of the right atrial isthmus in patients with isthmus-dependent atrial flutter can be highly successful, recurrences and complications occur in some patients. Our study provides further morphological details for a better understanding of the structure of the isthmus.**

Methods and Results: **We examined the isthmic area in 30 heart specimens by dissection, histology, and scanning electron microscopy. This area was bordered anteriorly by the hinge of the tricuspid valve and posteriorly by the orifice of the inferior caval vein. With the heart in attitudinal orientation, we identified and measured the lengths of three levels of isthmus: paraseptal (24 $\pm$ 4 mm), central (19 $\pm$ 4 mm), and inferolateral (30 $\pm$ 3 mm). Comparing the three levels, the central isthmus had the thinnest muscular wall and the paraseptal isthmus the thickest wall. At all three levels, the anterior part was consistently muscular whereas the posterior part was composed of mainly fibro-fatty tissue in 63% of hearts. The right coronary artery was less than 4 mm from the endocardial surface of the inferolateral isthmus in 47% of hearts. Inferior extensions of the atrioventricular node were present in the paraseptal isthmus in 10% of hearts, at 1–3 mm from the endocardial surface.**

Conclusions: **The thinner wall and shorter length of the central isthmus together with its distance from the right coronary artery, and nonassociation with the atrioventricular node or its arterial supply, should make it the preferred site for linear radiofrequency ablation.** *(J Cardiovasc Electrophysiol, Vol. 16, pp. 402-408, April 2005)*

ablation, atrial flutter, atrioventricular node, flutter isthmus, morphology

Introduction

The inferior right atrial cavo-tricuspid isthmus, a critical link for the macro-reentrant circuit of isthmus-dependent atrial flutter, is the target of catheter ablation techniques that have become the treatment of choice for this arrhythmia.[1-3] Creation of a complete bidirectional conduction block across the isthmus is the accepted electrophysiological ablation endpoint for long-term success but its achievement may be difficult or temporary in some patients.[4-9] In addition, experimental animal studies have demonstrated that a transmural lesion of the atrial wall is required to achieve ablation success.[10-12] The ease of obtaining a complete, transmural, and permanent isthmus ablation line depends on architectural factors of the inferior isthmus such as its size, endocardial geometry, and content of myocardial and fibro-fatty tissues at the ablation zone.[13-18] Ablation catheters with irrigated or large-tip electrodes, producing deeper lesions than conventional 4-mm tip electrodes, are now standard for the ablation of isthmus-dependent atrial flutter.[19-26] Reported rates of atrial flutter recurrences with these new ablation techniques are variable, but in some centers they may be as high as 10%.[27-28] Cryoablation of atrial flutter, although less painful than radiofrequency catheter techniques,[29-30] is followed by an 11% recurrence rate of the arrhythmia after an apparent acute bidirectional isthmic block.[30]

Apart from success and recurrence rate, additional issues for isthmic catheter ablation in patients with atrial flutter are the production of pain,[29] and the possibility of damaging elements of the normal AV nodal conduction pathway,[31] or the neighboring vasculature,[32-33] and the regional innervation. The gross morphological features of the inferior isthmus have been described in postmortem specimens recognizing the existence of sectors with a variable content of myocardium and fibro-fatty tissue.[13,14] However, architectural details on the relations among the possible target areas for ablation with the underlying myocardial thickness, coronary vessels, nerve endings, and elements of the atrioventricular node, remain to be examined. The present morphological and histological study was designed to provide these details for a better understanding of the target ablation areas in isthmus-dependent atrial flutter particularly in connection with current and emerging ablation techniques aimed at producing larger and deeper lesions in this region.

Address for correspondence: Siew Yen Ho, Ph.D., F.R.C.Path, F.E.S.C., Paediatrics, National Heart and Lung Institute, Imperial College, London SW3 6LY, UK. Fax: ++44 20 7351 8230; E-mail: yen.ho@imperial.ac.uk

Funding received from Grant SAF2004-06864 (J.A.C. and D.S.Q.) from Ministerio de Educación y Ciencia, Spain, Fondo de Investigaciones dela Seguridad Social (Redes Temáticas de Cooperación; Red Cardiovascular C01/03) (J.A.F. and J.F.), and Royal Brompton and Harefield Hospital Charitable Fund (S.Y.H.).

Manuscript received 13 October 2004; Accepted for publication 27 October 2004.

doi: 10.1046/j.1540-8167.2005.40709.x

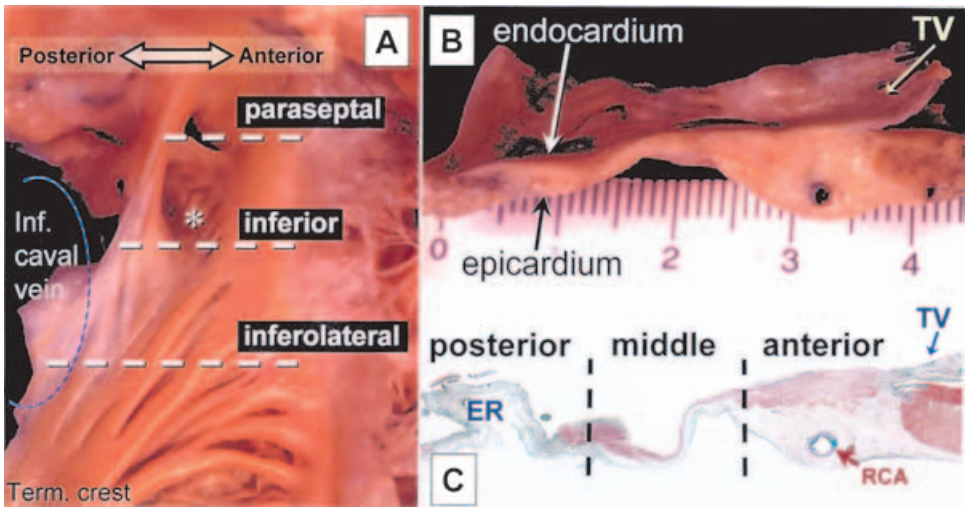

Figure 1. *A: The endocardial surface of the right atrial isthmus is displayed to show the three levels. Note the pouch at the central isthmus and the distal ramifications of the terminal (Term.) crest that feed into the inferolateral isthmus. B and C: The isthmus viewed in profile. The histological section shows myocardium in red and fibrous tissue in green. The anterior sector corresponds to the vestibule leading to the tricuspid valve (TV) and is related to the right coronary artery (RCA). The posterior sector is closest to the orifice of the inferior caval vein and contains the Eustachian valve or ridge (ER) [Masson's trichrome stain].*

Materials and Methods

We examined 30 formalin-fixed hearts from patients who died of noncardiac causes (21 males and 9 females, mean age 46 ± 22 years). The causes of death were traffic accident (15), lung and ovarian carcinoma (5), suicide (5), and cerebral hemorrhage (5). All hearts were structurally normal weighing 360 ± 40 g. The walls of the right atrium were dissected to display the isthmic area between the inferior caval vein and the tricuspid valve, which had an irregular quadrilateral shape (Fig. 1). When traced on heart specimens, we had previously distinguished three morphological sectors within the isthmus: the anterior smooth myocardial vestibule or pretricuspideal region, the middle trabeculated sector, and the posterior membranous sector adjacent to the Eustachian valve (Figs. 1 and 2).[13] The isthmic area was examined along three parallel levels described in attitudinal orientation as paraseptal isthmus, inferior isthmus, and inferolateral isthmus (Figs. 1 and 2).

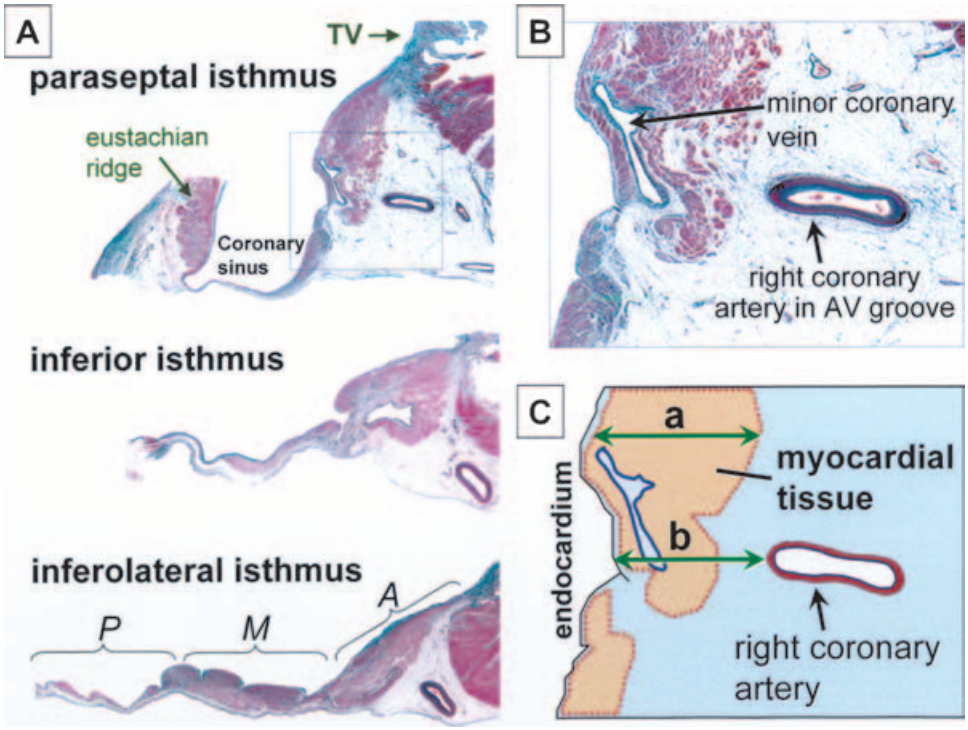

Figure 2. *A: The three levels of isthmus from a heart specimen that has a right dominant coronary artery. The boxed area is enlarged in B. B and C: illustrate the myocardial thickness (a) and distance between the endocardial surface and the right coronary artery (b). Note the minor coronary vein close to the endocardium. P, M, and A = posterior, middle, and anterior sectors, respectively [Masson's trichrome stain].*

The inferior isthmus is also known as the "central isthmus" owing to its location between the other two isthmuses on left anterior-oblique projection. Each level was delimited anteriorly by the hingeline of the tricuspid valve. Full thicknesses of the atrial wall at the isthmus area were prepared for light and scanning electron microscopic studies. The blocks were dehydrated in a graded series of ethanol, embedded in paraffin, and serially sectioned at 10 μm in a sagittal plane (15 blocks were sectioned in a frontal plane) that profiled the three morphological sectors in the same section along each of the three levels (Fig. 2A). Deparaffinized sections were stained with Masson's trichrome and van Gieson techniques at 1-mm intervals. We measured the wall thickness from endocardium to epicardium at the three morphological sectors. At every sector, the distance from endocardium to the most epicardial myocardial limit was also measured. In addition, we measured the minimal distances from the endocardium to the adventitia of the right coronary artery or minor coronary veins. We also measured the distances from the right atrial endocardium to the inferior extensions of the AV node and noted the presence of ganglia and fibers of the autonomic nervous system.

Statistical Study

Data are expressed as mean ± standard deviation. Quantitative data were compared using an unpaired *t*-test and P values less than 0.05 were considered significant.

Results

Gross Morphological Features of the Isthmic Area

The right atrium, as displayed in attitudinally simulated right anterior oblique projection, showed on its endocardial surface a quadrilateral-shaped isthmic area bordered by the tricuspid valve anteriorly and the Eustachian valve and ridge posteriorly (Fig. 1A). The superior border of the quadrangle is the paraseptal isthmus (so-called septal isthmus), which also marks the base of the triangle of Koch. The length of the paraseptal isthmus was 24 ± 4 mm (range 14–33 mm). The inferolateral border of the quadrilateral area contained the pectinate muscles, which were final ramifications of the terminal crest. Its length was 30 ± 3 mm (range 18–36 mm). The central zone of the isthmus, the inferior isthmus, is the where the inferior caval vein orifice is closest to the tricuspid valve insertion. It extended over 19 ± 4 mm (range 13–26 mm). In 25 of our specimens (83%) the central isthmus traversed through a recess, the subeustachian sinus (Fig. 1). The longest diameter of the mouth of the pouch-like recess measured 14 ± 3 mm and its depth was 2.9 ± 1.2 mm and deeper than 5 mm in two specimens. In the majority of specimens, the pouch was membranous (63%, 19 hearts), with scarce muscular fibers (Figs. 2 and 3).

Myocardial Thickness and Architecture of the Isthmic Region

Table 1 shows the myocardial thickness across the three isthmic levels and sectors. The central isthmus had the thinnest muscular wall across the sectors (anterior vestibular, inferior trabeculated, and posterior membranous) compared to the paraseptal and inferolateral isthmus (Table 1). In 23 specimens (77%), the posterior membranous and trabeculated sectors of the central isthmus were made up of longitudinal or obliquely arranged bundles of atrial myocardium separated by connective tissue (Fig. 3). The isthmus level with the thickest muscular content in all three sectors was the paraseptal isthmus. The inferolateral isthmus was intermediate in myocardial thickness.

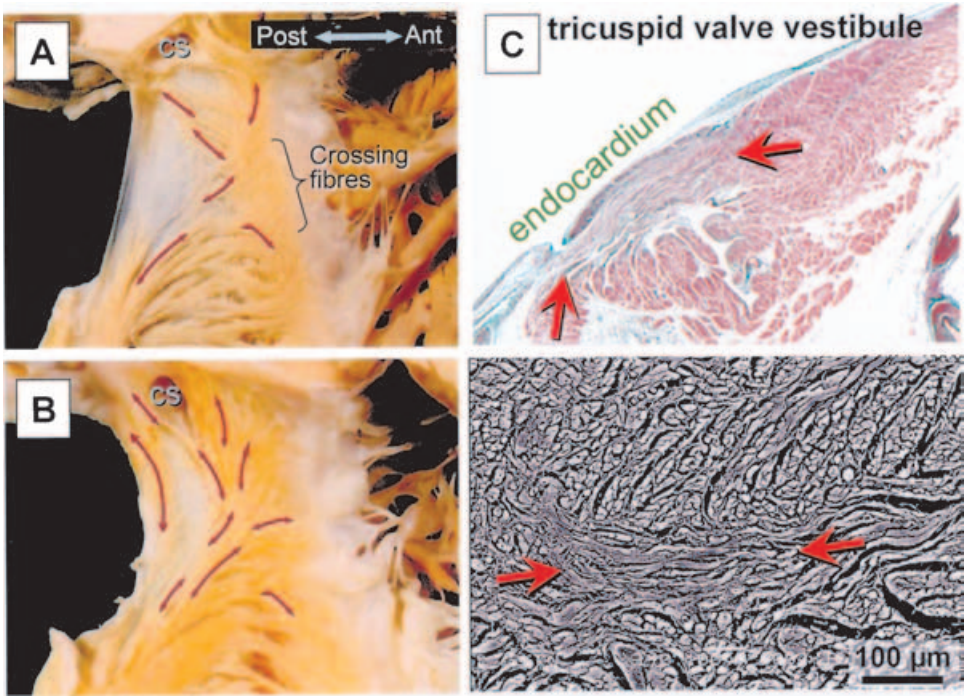

Figure 3. *A and B: are dissections of the endocardial surface showing the myofiber arrangement (double-headed arrows) and the pale areas that lack myocardium. C and D: are histologic and scanning electron micrographs, respectively, showing longitudinal myofibers (between arrows) intersecting circumferentially arranged myofibers in the vestibule (CS = coronary sinus; TC = terminal crest [Masson's trichrome stain]).*

TABLE 1

Mean Myocardial Thickness in mm (Range) Across the Three Levels and Sectors of the Isthmus

Level	Sector		
	Posterior Membranous	**Inferior Trabeculated**	**Anterior Smooth**
Paraseptal	3.1 ± 1.3 (1.1–6.9)	2.4 ± 1.1 (1.2–4.1)	4.3 ± 0.9 (2.5–6.1)
Central	1.2 ± 0.7 (0–2.3)*	0.8 ± 0.5 (0.2–3.1)**	3.5 ± 1.2 (1.2–6.1)***
Inferolateral	1.6 ± 0.9 (0.3–3.1)	1.7 ± 1.1 (0.5–3.1)	4.1 ± 1.2 (2.1–5.3)

*P < 0.001 versus paraseptal, *P < 0.1 versus inferolateral; **P < 0.001 versus paraseptal, **P < 0.01 versus inferolateral; ***P < 0.01 versus paraseptal, ***P < 0.1 versus inferolateral.

In terms of overall myocardial content of the isthmic region, the posterior membranous and middle trabeculated sectors in 19 of our specimens (63%) were composed of fibro-fatty tissue with sparse myocardial bundles 1.1–2.1 mm thick that extended from the terminal crest toward the Eustachian ridge to surround the mouth of the coronary sinus. In this region, the myocardial bundles blended into the left atrial myocardium along the proximal portion of the coronary sinus (Fig. 3A,B). Variations of this pattern were observed in 11 specimens (37%) that had the posterior and middle sectors extensively crossed by thick myocardial bundles 3–7-mm thick. Eight of these 11 specimens (26% of the total) had a prominent Eustachian ridge 3.2 ± 0.8 mm thick (range 2.1–4.3 mm) and a muscular Eustachian valve (Fig. 4A). Five of these 11 specimens (17% of the total) had a muscular Thebesian valve (Fig. 4A,B). The anterior smooth vestibular sector is consistently muscular with obliquely arranged bundles fibers terminating on the hinge of the tricuspid valve while others continued superiorly into the triangle of Koch. In the central isthmus, we found that in 18 hearts (60%) the obliquely or longitudinal muscle fibers passed from the middle sector to the anterior sector as the continuation of the distal ramifications of the terminal crest, or proceeded towards the region beneath the orifice of the coronary sinus. Within the vestibular sector, these fibers were crossed in the subendocardium by circumferentially arranged fibers in the paraseptal area (Fig. 3A,C,D). In 26 specimens (87%), the posterior membranous sector of the inferolateral isthmus consisted of densely packed myocardial bundles from the terminal crest (Figs. 1A and 3A,B). In the remaining four specimens, this sector was membranous showing extensive fibro-fatty tissue with scanty myocardial content.

In addition, we observed in most of the hearts (19 specimens, 63%) a fibrous endocardial thickening of 0.5 ± 0.2 mm in the vestibule of the isthmus compared to a mean thickness

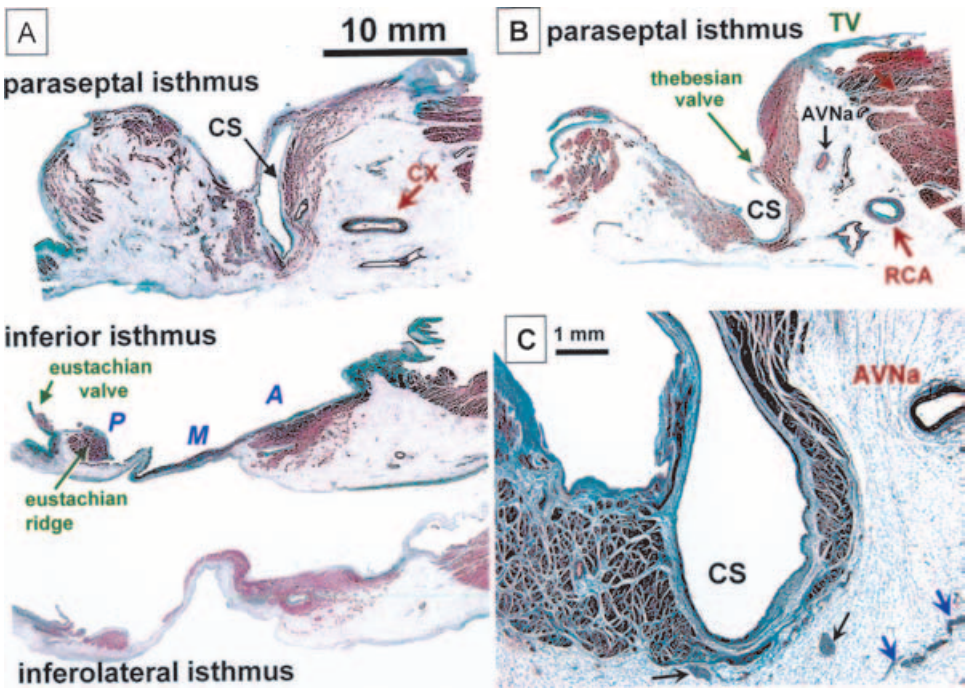

Figure 4. *A: This series of sections is through the three levels of isthmus from a heart with dominance of the left coronary artery. Note the muscular Thebesian valve guarding the coronary sinus (CS), prominent Eustachian ridge, and muscular Eustachian valve. The subendocardial connective tissue is thicker in the anterior sector than in the other two sectors. B: This paraseptal isthmus from a heart with right dominant coronary artery (RCA) includes the artery to the atrioventricular node (AVNa). C: This magnified view of a paraseptal isthmus shows parasympathetic ganglia (black arrows) and nerve bundles (blue arrows) close to the coronary sinus (CS). Note proximity of the atrioventricular nodal artery (AVNa) to the endocardial surface (CX = circumflex artery; P, M, and A = posterior, middle, and anterior sectors, respectively [Masson's trichrome stain]).*

TABLE 2
Mean Minimal Distance in mm (Range) Between Endocardium and Right Coronary Artery

Paraseptal isthmus	4.5 ± 2.3 (2–11)
Central isthmus	4.2 ± 2.1 (2–8)
Inferolateral isthmus	3.3 ± 1.1 (3–6)

of 0.2 ± 0.1 mm in the middle and posterior sectors at all levels of the isthmus.

Relation Between the Paraseptal Isthmus and the Specialized Atrioventricular Conduction System, Coronary Vessels, and the Autonomic Nervous System

At the paraseptal isthmus, we found in three specimens (10%) the inferior extensions of the compact atrioventricular node with histologically specialized characteristics around the artery supplying the atrioventricular node. At this level, the distances between the inferior nodal extensions to the endocardium ranged from 1 to 3 mm. At the central and inferolateral isthmic levels, the atrial myocytes did not show any histologically specialized characteristics reminiscent of extensions from the sinus or atrioventricular nodes.

The right coronary artery runs epicardially in the fat-filled atrioventricular groove and is related with the smooth anterior vestibular sector (Figs. 1, 2, and 4B). In five hearts (17%), the circumflex was the dominant coronary artery and it was seen only at the paraseptal level (Fig. 4A). Table 2 shows the minimal distances between the coronary artery and the endocardial surface. In 14 specimens (47%), at the inferolateral isthmus, the right coronary artery was less than 4 mm from the endocardium. The atrioventricular nodal artery arose from the right coronary artery in 25 hearts (83%) and from the circumflex artery in 5 hearts (17%). At the paraseptal level the artery passed through the pyramidal space close to the mouth of the coronary sinus (mean 3.2 ± 1.3 mm, range 0.3–4.4 mm) (Fig. 4A,B,C).

Minor coronary veins of variable diameters were evident in 25 hearts (83%). They ran intramyocardially in the vestibular sector of the inferolateral isthmus, parallel to the tricuspid annulus, posteriorly and superiorly to the right coronary artery, to reach the coronary sinus orifice at the paraseptal isthmus (Fig. 2B).

A small number of parasympathetic ganglia or fibers of the autonomic nervous system were found epicardially at the inferior and the paraseptal isthmic levels. They were most frequently seen in the inferior margin of the coronary sinus at the paraseptal isthmus (19 hearts, 63%) (Fig. 4C).

Discussion

Major Findings

Although previous anatomical and imaging studies have shown a range of morphologies and wall thicknesses in the isthmus,[13–18,34] the present study provides further morphological and histological information in the three levels of the isthmus and their anatomical relations with the coronary vessels and the inferior extensions of the compact atrioventricular node, thus providing a guide to designing more effective and safer ablation lines using new ablating tools. Our histological results, albeit on normal hearts, demonstrate for the first time, that the central/inferior isthmus (the 06:00 a.m. region in a fluoroscopic left anterior oblique view) is thinner along its entire length encompassing the three morphological sectors than the paraseptal and inferolateral isthmus. The paraseptal isthmus has the thickest wall, harbors the artery to the atrioventricular node and, in 10% of specimens, the inferior extensions of the node. Our study also showed the close proximity of the right coronary artery to the endocardium of the inferolateral isthmus (<4 mm in 47% of specimens). Furthermore, our observation that the posterior and middle sectors (at all three isthmic levels) mainly consisted of fibrous tissue with few myocytes in 63% of specimens, suggests that the length of the isthmus that needs to be ablated, i.e., the conducting isthmus, can be considerably narrower than the area bounded by the anatomic barriers of the tricuspid valve anteriorly and the inferior caval vein posteriorly.

Myocardial Thickness of the Isthmus and Resistance to Catheter Ablation

In some patients with common atrial flutter, the ablation of the inferior isthmus may be difficult requiring many radiofrequency energy applications and long procedural times. With right atrial angiography it has been found that "difficult cases" had an enlarged inferior isthmus and a well-developed pouch-like posterior recess.[16,18] Right atrial angiography accurately defines the isthmus anatomy and may facilitate ablation in difficult cases.[15,18] In addition, phased-array intracardiac echocardiography may be used to characterize the variable wall thickness and to monitor the wall lesions during radiofrequency applications.[34]

Our present study shows that the musculature at the paraseptal isthmus is thicker in all its three sectors (posterior, middle, and anterior) than the central and inferolateral isthmus. This observation may account for some of the difficulties and recurrences noted in clinical series. In patients with atrial flutter, Fisher et al.[35] using criteria of noninducibility after ablation of typical atrial flutter, reported on success rates of 40% when the line of ablation was performed between the tricuspid annulus and the coronary sinus ostium (the paraseptal isthmus) as compared with 70% when the ablation line was traced from the caval vein to tricuspid annulus (central and inferolateral isthmus). Furthermore, in a prospective and randomized study using a 4-mm tip electrode catheter, Anselme et al.[36] compared the results of radiofrequency ablation at the paraseptal isthmus (between the Eustachian crest, the coronary sinus, and tricuspid annulus) named by the authors as "posterior side" of the isthmus, and the inferolateral isthmus (between the inferior vena cava and the tricuspid annulus) termed "anterior side" of the isthmus. They noted fewer number of radiofrequency pulses and shorter fluoroscopy times when the inferolateral isthmus was selected as the initial ablation target.[36] A thicker musculature with frequent muscular bundles at the paraseptal isthmus together with a prominent and muscular Eustachian ridge such as found in 26% of our specimens may require more radiofrequency energy lesions to complete the ablation line and also require difficult angling of the catheter for good contact. In addition, we found ganglia and fibers of autonomic nervous system at the epicardial region, which may explain the frequent complaint of pain experienced by patients when radiofrequency pulses are delivered in the inferior margin of the coronary sinus.

Shah et al.[37] using a 3D electroanatomic mapping of the isthmus analyzed the presence of "gaps" or remnant tissue from ablated areas. In their study, the ablation line was performed between the 5:30 to the 6:30 a.m. position in the fluroscopic left anterior oblique projections and gaps through the ablation line were situated near the edge of the tricuspid annulus in six patients and near the edge of the inferior caval vein in three. Others have located the most commonly occurring gaps in the vestibule of the tricuspid valve. [38] We have observed that the vestibular sector consistently has more musculature than the middle or posterior sectors, a feature that could account for the more frequent occurrence of post-ablation gaps at this area. In addition, a large intramyocardial "minor coronary vein" usually found at the vestibular sector may produce intramural cooling effects that reduce the efficacy of ablative energy. Fuller and Wood [39] have shown that flow through even small intramyocardial vessels can prevent transmural lesion formation and preserve conduction through a radiofrequency lesion. Recently, a histopathologic examination in a patient who had undergone an isthmus ablation showed that preserved myocardial cells were distributed along a small cardiac vein, lending support to the concept of blood flow having a protective effect on surrounding atrial myocardium.[40]

Risk of Inducing AV Block During Ablation in the Isthmic Area

Recently, new ablation catheters with longer or saline irrigated tip electrodes have been shown to produce deeper and larger isthmic lesions that can facilitate isthmus ablation and procedural success.[20-24] The irrigated-tip catheter can produce a continuous and larger transmural lesion 1–6 cm along the isthmus to a depth of 8 mm.[25] Theoretically, this can increase the risk of damaging the right coronary artery, the artery supplying the atrioventricular node or the inferior extensions of the node, with the consequence of inducing heart block. Our present histological study shows the close proximity of the right coronary artery to the endocardium, with a distance less than 4 mm in 47% of hearts. Madrid et al.[21] analyzed the effects on right coronary artery after isthmic ablation using an irrigated tip catheter in 16 pigs and only found 2 cases of focal inflammation without endothelium involvement or necrosis. A case report on a patient who had isthmic ablation with 8-mm tip catheter disclosed intramural hemorrhage adjacent to the side of the lesion, but no apparent injury of other layers of the arterial wall.[11] Right coronary angiograms performed before and after the ablation procedures in 30 patients treated by irrigated-tip catheter did not show changes in the right coronary artery, but the operators also took care to stay away from the paraseptal isthmus and the coronary sinus because of the proximity to the atrioventricular conduction system and thin-walled coronary veins.[20] The atrial musculature at the paraseptal isthmus is part of the posteroinferior input toward the atrioventricular node. In the present study, we found inferior extensions of the node in the paraseptal isthmus of three specimens (10%). Anselme et al.[36] reported that among the 42 patients in whom ablation was attempted at the paraseptal isthmus, transient atrioventricular block was documented in 5 patients (12%), and permanent atrioventricular block in 1 patient (2.4%). These incidences concur with other published series.[41,42] Atrioventricular block may be the consequence of direct damage to atrionodal inputs or the inferior nodal extensions,[31,43,44] or trauma to the nodal artery.[32,33,45]

Limitations

This is an anatomic study on structurally normal hearts and is without electrophysiological correlates. Materials for correlative studies are rarely available.[11,32,40] Our study, nevertheless, serves to provide anatomical details relevant to clinical practice.

Conclusions

Our anatomic finding showed a nonuniform myocardial thickness of the inferior right atrial isthmus. Of the three levels of the isthmus, the thinner wall and shorter length of the central/inferior isthmus should make it the preferred isthmus for constructing a complete linear line with radiofrequency ablation. In contrast, the paraseptal isthmus has the thickest wall, is close to the arterial branch supplying the atrioventricular node and, in some cases, can contain the inferior extensions of the node. The inferolateral isthmus is the longest and is in closest proximity to the right coronary artery.

References

1. Klein GJ, Guiraudon GM, Sharma AD, Milstein S: Demonstration of macroreentry and feasibility of operative therapy in the common type of atrial flutter. Am J Cardiol 1986;57:587-91.
2. Feld GK, Fleck RP, Chen PS, Boyce K, Bahnson TD, Stein JB, Calisi CM, Ibarra M: Radiofrequency catheter ablation for the treatment of human type 1 atrial flutter: Identification of a critical zone in the reentrant circuit by endocardial mapping techniques. Circulation 1992;86:1233-1240.
3. Cosio FG, Lopez Gil M, Goicolea A, Arribas F, Barroso JL: Radiofrequency ablation of the inferior vena cava-tricuspid valve isthmus in common atrial flutter. Am J Cardiol 1993;71:705-709.
4. Poty H, Saoudi N, Aziz AA, Nair M, Letac B: Radiofrequency ablation of type 1 atrial flutter: Prediction of late success by electrophysiological criteria. Circulation 1995;92:1389-1392.
5. Cauchemez B, Haissaguerre M, Fischer B, Thomas O, Clémenty J, Coumel P: Electrophysiological effects of catheter ablation on inferior vena cava-tricuspid annulus isthmus in common atrial flutter. Circulation 1996;93:284-294.
6. Poty H, Saoudi N, Nair M, Anselme F, Letac B: Radiofrequency catheter ablation of atrial flutter. Further insights into the various types of isthmus block: Application to ablation during sinus rhythm. Circulation 1996;94:3204-13.
7. Schwartzman D, Callans DJ, Gottlieb CD, Dillon SM, Movsowitz C, Marchlinski FE: Conduction block in the inferior vena caval-tricuspid valve isthmus: Association with outcome of radiofrequency ablation of type I atrial flutter. J Am Coll Cardiol 1996;28:1519-1531.
8. Schumacher B, Pfeiffer D, Tebbenjohanns J, Lewalter T, Jung W, Luderitz B: Acute and long-term effects of consecutive radiofrequency application on conduction properties of the subeustachian isthmus in type I atrial flutter. J Cardiovasc Electrophysiol 1998;9:152-163.
9. Tai CT, Chen SA, Chiang CE, Wen ZC, Huang JL, Chen YJ, Yu WC, Feng AN, Lin YJ, Ding YA, Chang MS: Long term outcome of radiofrequency catheter ablation for typical atrial flutter: Risk of prediction of recurrent arrhythmias. J Cardiovasc Electrophysiol 1998;9:115-121.
10. Tabuchi T, Okumura K, Matsunaga T, Tsunoda R, Jougasaki M, Yasue H: Linear ablation of the isthmus between the inferior vena cava and tricuspid annulus for the treatment of atrial flutter. A study in the canine atrial flutter model. Circulation 1995;92:1312-1319.
11. Leonelli FM, Natale A, O'Connor W: Human histopathologic findings following radiofrequency ablation of the tricuspid-inferior vena cava itshmus. J Cardiovasc Electrophysiol 1999;10:599-602.
12. Kohno I, Ishihara T, Umetani K, Sawanobori T, Ijiri H, Komori S, Tamura K: Pathological findings of the isthmus between the inferior vena cava and tricuspid annulus ablated by radiofrequency application. PACE 2000;23:921-923.

13. Cabrera JA, Sanchez-Quintana D, Ho SY, Medina A, Anderson RH: The architecture of the atrial musculature between the orifice of the inferior caval vein and the tricuspid valve. J Cardiovasc Electrophysiol 1998;9:1186-1195.
14. Waki K, Saito T, Becker AE: Right atrial flutter isthmus revisited: Normal anatomy favors nonuniform anisotropic conduction. J Cardiovasc Electrophysiol 2000;11:90-94.
15. Cabrera JA, Sánchez-Quintana D, Ho SY, Medina A, Wanguemert F, Gross E, Grillo J, Hernández E, Anderson RH: Angiographic anatomy of the inferior right atrial isthmus in patients with and without history of common atrial flutter. Circulation 1999;99:3017-3023.
16. Heidbuchel H, Willems R, van Rensburg H, Adams J, Ector H, Van de Werf F: Right atrial angiographic evaluation of the posterior isthmus: relevance for ablation of typical atrial flutter. Circulation 2000;101:2178-2184.
17. Schumacher B, Wolpert C, Lewalter T, Vahlhaus C, Jung W, Luderitz B: Predictors of success in radiofrequency catheter ablation of atrial flutter. J Interv Card Electrophysiol 2000;4(Suppl 1):121-125.
18. Da Costa A, Faure E, Thévenin J, Messier M, Bernard S, Abdel K, Robin C, Romeyer C, Isaaz K: Effects of isthmus anatomy and ablation catheter on radiofrequency catheter ablation of the cavotricuspid isthmus. Circulation 2004;110:1030-1035.
19. Rodriguez LM, Nabar A, Timmermans C, Wellens HJ: Comparison of results of an 8-mm split-tip versus a 4-mm tip ablation catheter to perform radiofrequency ablation of type I atrial flutter. Am J Cardiol 2000;85:109-112.
20. Jais P, Shah DC, Haissaguerre M, Hocini M, Garrigue S, Le Metayer P, Clementy J: Prospective randomized comparison of irrigated-tip versus conventional-tip catheters for ablation of common flutter. Circulation 2000;101:772-776.
21. Madrid AH, Rebollo JM, Del Rey JM, Gonzalo P, Socas A, Alvarez T, Rodriguez A, Correa C, Chercoles A, Vazquez C, Garcia-Cosio M, Palacios F, Moro C: Randomized comparison of efficacy of cooled tip catheter ablation of atrial flutter: Anatomic versus electrophysiological complete isthmus block. Pacing Clin Electrophysiol 2001;24:1525-1533.
22. Tsai CF, Tai CT, Yu WC, Chen YJ, Hsieh MH, Chiang CE, Ding YA, Chang MS, Chen SA: Is 8-mm more effective than 4-mm tip electrode catheter for ablation of typical atrial flutter? Circulation 1999;100:768-771.
23. Demazumder D, Mirotznik MS, Schwartzman D: Comparison of irrigated electrode designs for radiofrequency ablation of myocardium. J Interv Card Electrophysiol 2001;5:391-400.
24. Schreieck J, Zrenner B, Kumpmann J, Ndrepepa G, Schneider MA, Deisenhofer I, Schmitt C: Prospective randomized comparison of closed cooled-tip versus 8-mm-tip catheters for radiofrequency ablation of typical atrial flutter. J Cardiovasc Electrophysiol 2002;13:980-985.
25. Scavee C, Jais P, Hsu LF, Sanders P, Hocini M, Weerasooriya R, Macle L, Raybaud F, Clementy J, Haissaguerre M: Prospective randomised comparison of irrigated-tip and large-tip catheter ablation of cavotricuspid isthmus-dependent atrial flutter. Eur Heart J 2004;25:963-969.
26. Feld G, Wharton M, Plumb V, Daoud E, Friehling T, Epstein L: EPT-1000 XP Cardiac Ablation System Investigators. Radiofrequency catheter ablation of type 1 atrial flutter using large-tip 8- or 10-mm electrode catheters and a high-output radiofrequency energy generator: Results of a multicenter safety and efficacy study. J Am Coll Cardiol 2004;43:1466-1472.
27. Spitzer SG, Karolyi L, Rammler C, Otto T: Primary closed cooled tip ablation of typical atrial flutter in comparison to conventional radiofrequency ablation. Europace 2002;4:265-271.
28. Marrouche NF, Schweikert R, Saliba W, Pavia SV, Martin DO, Dresing T, Cole C, Balaban K, Saad E, Perez-Lugones A, Bash D, Tchou P, Natale A: Use of different catheter ablation technologies for treatment of typical atrial flutter: Acute results and long-term follow-up. Pacing Clin Electrophysiol 2003;26:743-746.
29. Timmermans C, Ayers GM, Crijns HJ, Rodriguez LM: Randomized study comparing radiofrequency ablation with cryoablation for the treatment of atrial flutter with emphasis on pain perception. Circulation 2003;107:1250-1252.
30. Manusama R, Timmermans C, Limon F, Philippens S, Crijns HJ, Rodriguez LM: Catheter-based cryoablation permanently cures patients with common atrial flutter. Circulation 2004;109:1636-1639.
31. Tai CT, Tsai CF, Hsieh MH, Lin WS, Lin YK, Lee SH, Yu WC, Ding YA, Chang MS, Chen SA: Effects of cavotricuspid isthmus ablation on atrioventricular node electrophysiology in patients with typical atrial flutter. Circulation 2001;104:1501-1505.
32. Weiss C, Becker J, Hoffmann M, Willems S: Can radiofrequency current isthmus ablation damage the right coronary artery? Histopathological findings following the use of a long (8 mm) tip electrode. Pacing Clin Electrophysiol 2002;25:860-862.
33. Ouali S, Anselme F, Savouré A, Savoure A, Cribier A: Acute coronary occlusion during radiofrequency catheter ablation of typical atrial flutter. J Cardiovasc Electrophysiol 2002;13:1047-1049.
34. Morton JB, Sanders P, Davidson N, Sparks P, Vohra J, Kalman J: Phased-array intracardiac echocardiography for defining cavotricuspid isthmus anatomy during radiofrequency ablation of typical atrial flutter. J Cardiovasc Electrophysiol 2003;14:591-597.
35. Fischer B, Haissaguerre M, Garrigues S, Poquet F, Gencel J, Clementy J, Marcus FI: Radiofrequency catheter ablation of common atrial flutter in 80 patients. J Am Coll Cardiol 1995;25:1365-1372.
36. Anselme F, Klug D, Scanu P, Poty H, Lacroix D, Kacet S, Cribier A, Saoudi N: Randomized comparison of two targets in typical atrial flutter ablation. Am J Cardiol 2000;85:1302-1307.
37. Shah D, Haissaguerre MK, Jais P, Takahaski A, Hocini M, Clementy J: High-density mapping activation through an incomplete isthmus ablation line. Circulation 1999;99:211-215.
38. Sra J, Bhatia A, Dhala A, Blanck Z, Rathod S, Boveja B, Deshpande S, Cooley R, Akhtar M: Electroanatomic mapping to identify breakthrough sites in recurrent typical human flutter. PACE 2000;23:1479-1492.
39. Fuller IA, Wood MA: Intramural coronary vasculature prevents transmural radiofrequency lesion formation: Implications for linear ablation. Circulation 2003;107:1797-1803.
40. Igawa O, Masamitsu A, Hisatome I, Matsui Y: Histopathologic background for resistance to conventional catheter ablation of common atrial flutter. J Cardiovasc Electrophysiol 2004;15:829-832.
41. Jackman WM, Beckman KJ, McClelland JH, Wang X, Friday KJ, Roman CA, Moulton KP, Twidale N, Hazlitt HA, Prior MI, Oren J, Overholt ED, Lazzara R: Treatment of supraventricular tachycardia due to atrioventricular nodal reentry by radiofrequency catheter ablation of slow pathway conduction. N Engl J Med 1992;327:313-318.
42. Calkins H, Yong P, Miller JM, Olshansky B, Carlson M, Saul JP, Huang SKS, Liem LB, Klein LS, Moser SA, Bloch DA, Guillete P, Prytowsky E, for the Atakr Multicenter Investigator Group: Catheter ablation of accessory pathways, atrioventricular nodal re-entrant tachycardia, and the atrioventricular junction. Final results of a prospective multicenter clinical trial. Circulation 1999;19:262-270.
43. Sánchez-Quintana D, Davies DW, Ho SY, Oslizlok P, Anderson RH: Architecture of the atrial Musculature in and around the triangle of Koch: Its potential relevance to atrioventricular nodal reentry. J Cardiovasc Electrophysiol 1997;8:1396-1407.
44. Inoue S, Becker AE: Posterior extensions of the human compact atrioventricular node. A neglected anatomic feature of potential clinical significance. Circulation 1998;87:188-193.
45. Khanal S, Ribeiro PA, Platt M, Kuhn MA: Right coronary artery occlusion as a complication of accessory pathway ablation in a 12-year-old treated with stenting. Catheter Cardiovasc Interv 1999;46:59-61.